RSC Sustainability

ROYAL SOCIETY OF CHEMISTRY

PAPER

View Article Online
View Journal | View Issue

Cite this: *RSC Sustainability*, 2024, **2**, 3345

Novel CO_2-philic porous organic polymers synthesized in water: a leap towards eco-sustainability†

Riccardo Mobili, ‡[a] Yue Wu, [b] Charl Xavier Bezuidenhout, [c] Sonia La Cognata, [a] Silvia Bracco, *[c] Mariolino Carta *[b] and Valeria Amendola *[a]

Received 14th August 2024
Accepted 11th October 2024

DOI: 10.1039/d4su00479e

rsc.li/rscsus

We introduce two novel keto-enamine-linked porous organic polymers (POPs) distinguished by the presence of methyl or ethyl groups in their triamine precursors. These innovative POPs can be synthesized efficiently in water under mild conditions, utilizing starting materials that can be prepared on a gram scale through well-established procedures. Unlike most CO_2-philic POPs, which often require organic solvents, high temperatures, catalysts, additives, or hydrothermal equipment, these new polymers are synthesized in pure water at a relatively low temperature (70 °C) without any catalysts or additives and using common glassware. The N-rich composition of these porous organic polymers also contributes to their high adsorption selectivity for CO_2 over N_2, as calculated with the IAST method at 298 K. This combination of environmentally friendly synthesis, high yield, and superior adsorption properties positions these novel POPs as promising candidates for greener carbon capture technologies based on solid sorbents.

Sustainability spotlight

The increasing concentration of greenhouse gases in the atmosphere, primarily CO_2, is a major concern in our time. Consequently, developing and implementing technologies for efficient carbon capture and reuse is an imperative task. Various technologies have been developed to achieve this goal, including adsorption techniques utilizing CO_2-philic sorbents such as porous organic polymers (POPs). In this study, we report the synthesis in water and the gas adsorption properties of two CO_2-selective keto-enamine POPs. The reported protocol not only avoids the use of catalysts or additional additives but also directly produces a material with permanent porosity, representing an easy and green process for producing POPs for the selective sorption and separation of CO_2 from gas mixtures. Our work emphasizes the importance of the following UN Sustainable Development Goals: Affordable and Clean Energy (SDG 7), Industry, Innovation, and Infrastructure (SDG 9), and Climate Action (SDG 13).

Introduction

The increasing amount of greenhouse gases in the atmosphere (mostly CO_2) is a major concern in our times. With an annual release of more than 32 gigatons (Gt), the accumulation of anthropogenic carbon dioxide in the atmosphere has led to a 0.8–1.2 °C increase in global temperatures compared to pre-industrial levels. Global warming is considered the cause of a myriad of natural calamities, posing threats to the environment and human health.[1] Consequently, developing and implementing new technologies for efficient Carbon Capture Utilization and Storage (CCUS) systems are imperative tasks. Various technologies have been developed to selectively remove CO_2 from gas mixtures. Examples include chemical absorption in alkanolamine solutions,[2] membrane separation,[3] and adsorption-based techniques.[4] In the latter approach, solid sorbents that can selectively interact with a gas species through physical interactions are employed. A wide range of extended or molecular porous materials have been explored for this purpose, including zeolites and porous carbon,[5] Metal–Organic Frameworks (MOFs),[6] molecular materials such as Porous Organic Cages (POCs),[7] and others.[8] Promising alternatives for CO_2 capture and separation include Porous Organic Polymers (POPs),[9] Covalent Organic Frameworks (COFs),[10] Polymers of Intrinsic Microporosity (PIMs),[11] and Conjugated Microporous Polymers (CMPs),[12] among others.[13] POPs comprise organic

[a]*Department of Chemistry, University of Pavia, Viale Tarquato Taramelli 12, Pavia, 27100, Italy. E-mail: valeria.amendola@unipv.it*

[b]*Department of Chemistry, Faculty of Science and Engineering, Swansea University, Singleton Park, Swansea, Wales, SA2 8PP, UK. E-mail: mariolino.carta@swansea.ac.uk*

[c]*Department of Materials Science, University of Milano-Bicocca, Via Cozzi 55, Milano, 20125, Italy. E-mail: silvia.bracco@unimib.it*

† Electronic supplementary information (ESI) available: Materials and methods; synthetic procedures; details on physico-chemical characterization and spectra of the synthesized polymers; gas adsorption studies. See DOI: https://doi.org/10.1039/d4su00479e

‡ Present address: Sorbonne Université, CNRS, Institut Parisien de Chimie Moléculaire, 4 Place Jussieu, 75005 Paris, France.

linkers containing lightweight elements (*e.g.*, C, H, B, N, O) held together by covalent bonds. These materials typically exhibit high porosity, thermal and chemical stability, and allow easy tuning of pore size and functionalities.[14] Due to these characteristics, POPs have shown great potential in various applications such as catalysis,[15] chemical sensing,[16] energy storage,[17] and, notably, gas storage and separation.[9,18] Furthermore, the presence of heteroatoms in the backbone structure, particularly nitrogen, is well known to promote selective CO_2 capture through dipole–quadrupole interactions.[19] Schiff base condensation is a well-established process in the synthesis of CO_2-philic POPs. Critical issues connected to the susceptibility of Schiff bases to hydrolysis have successfully been addressed by converting imine bonds into more robust linkages, *e.g.*, keto-enamines. For porous organic materials, this is achieved by reacting primary polyamines with 1,3,5-triformylphloroglucinol (TFP).[19,20] In fact, the Schiff base formed undergoes an irreversible keto–enol tautomerization, leading to a keto-enamine product that is stabilized by intramolecular H-bonds.[19] Apart from a few examples of keto-enamine-based COFs obtained through mechanochemical solid state synthesis,[19c] most of the currently applied syntheses for CO_2-philic POPs involve the use of toxic organic solvents (*e.g.*, dioxane, mesitylene, dimethylformamide, *o*-dichlorobenzene and other halogenated solvents), acidic or metal catalysts, and high reaction temperatures (100–200 °C).[9] It is, therefore, crucial to develop more environmentally friendly procedures for synthesizing POPs in order to facilitate the future industrial applications of these porous materials in CO_2 sorption.[21] While water represents a greener alternative as a solvent for synthesizing POPs, there are still limited examples of its efficient utilization.[9,21–26]

In this study, we report the syntheses in water and the gas adsorption properties of two novel CO_2-philic keto-enamine POPs: POP-W-Et and POP-W-Me (Scheme 1). The optimized protocol for forming these nitrogen-rich polymers involves the condensation between non-planar, water-soluble tris-amines [1,3,5-tris(aminomethyl)mesitylene and 1,3,5-tris(aminomethyl)-2,4,6-triethylbenzene] and 1,3,5-triformylphloroglucinol, conducted without the need for acidic or transition metal-based catalysts, and under mild reaction conditions. The resulting amorphous keto-enamine-based polymers have been comprehensively characterized and assessed for gas adsorption applications, with a particular focus on the selectivity for CO_2 over N_2. Additionally, the novel POPs have been compared with the same polymers obtained under conventional conditions (using organic solvents and acid catalysts) to determine whether the water-based synthesis affects the physicochemical characteristics and the adsorption properties of the materials.

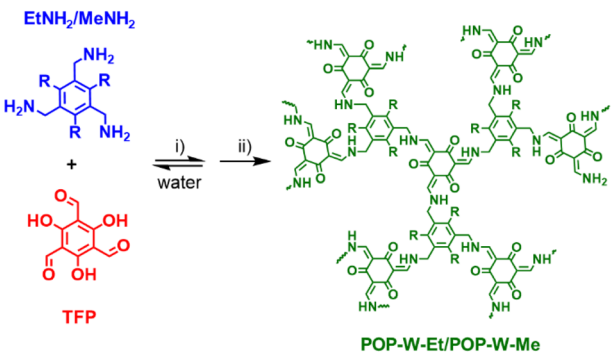

Scheme 1 Synthesis of porous organic polymers POP-W-Me and POP-W-Et in water (R = methyl and ethyl groups, respectively). The Schiff base condensation (i) was conducted at 70 °C for 3 days, without any catalyst or additive, using either 1,3,5-tris(aminomethyl)mesitylene and 1,3,5-tris(aminomethyl)-2,4,6-triethylbenzene (*i.e.* $MeNH_2$ and $EtNH_2$) as the tris-amine reagents. The condensation is followed by the irreversible keto–enol tautomerism (ii) yielding the final POP-W-Me and POP-W-Et β-keto-enamine polymers.

Results and discussion

Synthesis of the novel keto-enamine POPs

POP-W-Et and POP-W-Me were synthesized in aqueous solution ('W' indicates that the reaction was conducted in water) through one to one Schiff base condensation between 1,3,5-triformylphloroglucinol (TFP) and two distinct non-planar, water-soluble tris-amines, 1,3,5-tris(aminomethyl)mesitylene and 1,3,5-tris(aminomethyl)-2,4,6-triethylbenzene (named $MeNH_2$ and $EtNH_2$ for simplicity). All the starting compounds ($EtNH_2$, $MeNH_2$, TFP) were synthesized on a gram scale following procedures already reported in the literature (see the ESI section†).

Our study started by optimizing the synthetic conditions: reaction time, temperature, and presence/absence of acetic acid as a catalyst. $EtNH_2$ was chosen as the model amine at this stage, given that its homologue (*i.e.*, $MeNH_2$) demonstrated comparable reactivity and water solubility. Five polymer samples (s1–s5) were obtained for POP-W-Et, in diverse conditions reported in Table 1. This investigation pointed out that variations in reaction temperature (room temperature *vs.* 70 °C) and reaction time (24 hours *vs.* 72 hours) had low impact on reaction yields and surface areas. On the other hand, the presence of an acid catalyst negatively impacted the porosity of the materials. This observation aligns with the findings of J. Lu *et al.*,[27] who reported that azine-linked COFs could be efficiently synthesized in water (72 hours, 120 °C) in the absence of acetic acid as a catalyst. Compared to most of the previously reported examples,[9a] the polymers synthesized in this work were obtained in larger yield (90%) by reacting in water without any catalyst (or other additives) at a lower reaction temperature (70 °C). The sample featuring the highest surface area is POP-W-Et_s4 (Table 1).

We also synthesized the POPs using more conventional conditions, such as a 1,4-dioxane/mesitylene 4 : 1 (v/v) mixture, to compare and validate the efficacy of the water-based synthesis. The results for the two polymer samples, POP-O-Et_s1 and POP-O-Et_s2, are shown in Table 1 ('O' indicates the use of the organic solvent mixture). On the contrary of our previous findings in water, using acetic acid as a catalyst proved crucial for achieving high specific surface areas, such as for POP-O-Et_s2 synthesized at 70 °C for 72 hours with an 85% yield.

Table 1 Optimization of reaction conditions for the formation of POP-W-Et and POP-O-Et. The best conditions were those of POP-W-Et_s4 and POP-O-Et_s2 samples, referred to as POP-W-Et and POP-O-Et, for simplicity in the main text

Sample (S)	Solvent	Catalyst	Temperature (°C)	Time (h)	Yield (%)	SA_{BET}[a] ($m^2\ g^{-1}$)	SA_{BET}[b] ($m^2\ g^{-1}$)
POP-W-Et_s1	H_2O	—	r.t.	24	93	321	—
POP-W-Et_s2	H_2O	AcOH	r.t.	24	87	176	—
POP-W-Et_s3	H_2O	—	70	24	83	344	—
POP-W-Et_s4	H_2O	—	70	72	90	344	389
POP-W-Et_s5	H_2O	AcOH	70	24	73	182	—
POP-O-Et_s1	Dioxane/mesitylene 4 : 1	—	70	72	70	253	—
POP-O-Et_s2	Dioxane/mesitylene 4 : 1	AcOH	70	72	85	454	440
POP-O-Me	Dioxane/mesitylene 4 : 1	AcOH	70	72	92	227	302
POP-W-Me	H_2O	—	70	72	93	257	348

[a] The SA_{BET} was calculated from CO_2 adsorption curves at 273 K. [b] The SA_{BET} was calculated from CO_2 adsorption curves at 195 K.

The optimized reaction conditions (reported in the experimental section), corresponding to those employed for samples POP-W-Et_s4 and POP-O-Et_s2, were subsequently applied in the reactions of $MeNH_2$ with TFP, leading to the corresponding POP-W-Me and POP-O-Me polymers (Table 1). Before undergoing chemical and morphological characterization, the crude POPs were thoroughly washed with water, acetone, and methanol to eliminate any residual unreacted monomers or small oligomers. Subsequently, they were dried under vacuum at 80 °C for 24 hours.

Physico-chemical characterization

The novel POPs have been characterized by elemental analysis (Table S1†), Fourier Transform Infrared (FT-IR) and solid-state NMR spectroscopies, Powder X-ray diffraction (PXRD) and scanning electron microscopy (SEM). Moreover, thermal stability was assessed using Thermogravimetric analysis (TGA). POP-W-Et/POP-O-Et and POP-W-Me/POP-O-Me exhibited similar decomposition patterns, with a first mass loss initiating around 300 °C and a second starting at 400 °C, leading to complete sample degradation at approximately 650 °C. The patterns also display a slight mass loss below 100 °C, which can be attributed to residual solvent or adsorbed humidity (see Fig. S4–S7†), as observed in previously reported β-keto-enamine-based organic materials.[28] Differential Scanning Calorimetry (DSC) measurements on the POPs confirmed this hypothesis, showing that endothermic peaks at 55 °C have no counterpart in the cooling cycle (Fig. S8–S11†).

The FT-IR spectra exhibited similarities for all the investigated samples, regardless of whether they were synthesized in water or organic media.

Notably, the disappearance of the N–H stretching frequency for the tris-amines, the shift of the C=O peak to lower energy (from 1639 cm^{-1} in TFP to 1598 cm^{-1} in both POPs) and the emergence of prominent C=C peaks (at 1545 cm^{-1} for POP-W-Et/POP-O-Et; 1541 cm^{-1} for POP-W-Me/POP-O-Me) are consistent with the formation of the β-keto-enamine frameworks. This is further endorsed by the absence of stretching peaks corresponding to O–H and C=N bonds (Fig. S12–S13†), and by the presence of peaks due to C–N bonds at 1303 and 1309 cm^{-1} for POP-W-Et/POP-O-Et and POP-W-Me/POP-O-Me, respectively.[20]

Solid-state NMR spectroscopy confirmed the formation of the β-keto-enamine polymer frameworks. In particular, the ^{1}H–^{13}C Cross Polarization Magic Angle Spinning (CP MAS) spectra collected with the contact time of 2 ms exhibit several signals in complete agreement with the chemical structure of the monomeric unit, both for POP-W-Et and POP-W-Me (Fig. 1 and S14–S18†). Notably, the spectra do not display peaks around 192 ppm (ref. 20) due to residual or terminal aldehyde groups. Single peaks are observed for each species, except for the carbonyl (keto) group (*ca.* 185 ppm), which shows a more complex line shape, suggesting alternative configurations of the nearby enamine double bonds. Signal assignments were established by comparison to ^{1}H–^{13}C CPMAS experiments performed at shorter contact time (50 μs), which allows only the observation of carbon atoms directly bonded to hydrogen atoms. Additionally, ^{13}C Single Pulse Experiment spectra (SPE MAS) performed with a recycle delay of 60 s confirmed the formation of the expected chemical structures (Fig. S15, S17 and Table S2†).

Notably, no discernible differences have been found between materials synthesized in water and their counterparts produced in organic solvents, demonstrating that both synthetic

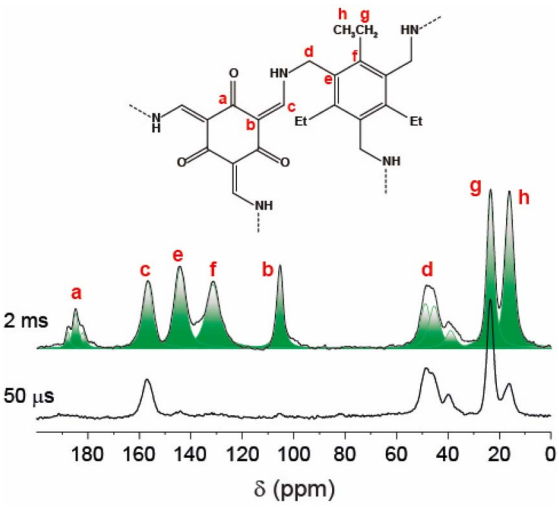

Fig. 1 ^{1}H–^{13}C CP MAS NMR spectra of POP-W-Et performed at variable contact time and a spinning speed of 12.5 kHz.

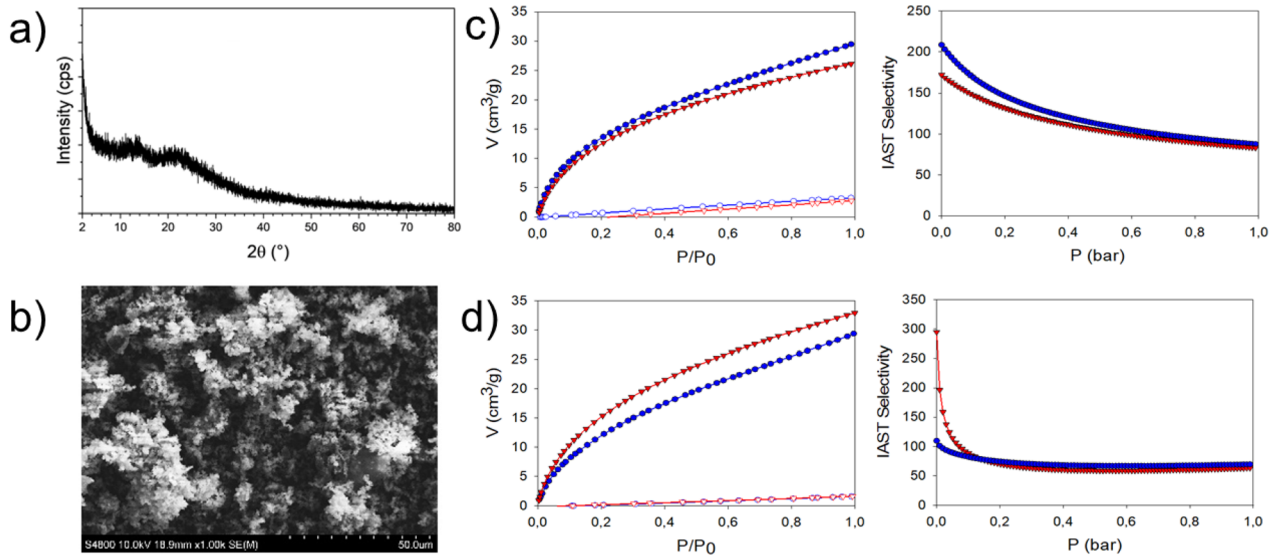

Fig. 2 (a) and (b), PXRD and SEM picture of POP-W-Et (see additional material in the ESI†). c) POP-W-Me (blue) and POP-O-Me (red): adsorption curves at 298 K of CO_2 and N_2 (full and empty symbols, respectively), and calculated IAST selectivity. (d) POP-W-Et (blue) and POP-O-Et (red): adsorption curves at 298 K of CO_2 and N_2 (full and empty symbols, respectively), and calculated IAST selectivity. The units for the adsorption plots are $cm^3\ g^{-1}$ STP.

strategies are perfectly feasible. PXRD analysis revealed that all the employed synthetic procedures yield amorphous materials, as demonstrated by the presence of two broad features at 14° (d = 6.3 Å) and 22° (d = 4.0 Å) for both POP-W-Et/POP-O-Et and POP-W-Me/POP-O-Me (Fig. 2 and S20–S23†). Scanning Electron Microscopy (SEM) investigations unveiled similar morphologies for the four POPs, characterized by aggregated globular-shaped particles with average dimensions of 0.5–1 μm. Remarkably, even in this case we found no significant differences between materials synthesized in water and those produced in organic media (Fig. 2 and S24–S25†).

The elemental composition of the two polymers was analysed, with the results presented in Table S1.† From these data, we can conclude that, although POP-Me exhibits a slightly higher nitrogen content (in both water and organic solvent), this does not appear to significantly impact the CO_2 uptake. Interestingly, the highest CO_2/N_2 selectivity (Table 2 and Fig. 2) was observed for POP-Et, despite the slightly greater presence of nucleophilic nitrogen in POP-Me, which would theoretically enhance CO_2 binding due to its Lewis acidity. In both cases (Et and Me), the polymers synthesised in water exhibited a slightly higher nitrogen content compared to those synthesized in the organic solvent, which may suggest a greater abundance of free amine end groups in the water-based synthesis and, potentially, indicating a lower degree of polymerization.

Nevertheless, the strong performance of the water-based synthesis yields results that are highly comparable to the organic solvent method and, in addition, offers a greener alternative.

Gas adsorption studies

As earlier mentioned, the optimization of synthesis was carried out considering the best balance between reaction yield and surface area of the individual polymer samples.

Before determining the surface area, the samples in Table 1 were activated by outgassing overnight at 350 K under dynamic vacuum to eliminate any traces of water in the materials. Gas adsorption studies were carried out on the activated materials using CO_2 and N_2 as probe gases. Initial efforts to determine the Brunauer–Emmett–Teller surface areas (SA_{BET}) using N_2 at 77 K proved unsuccessful due to very low nitrogen adsorption. The surface area of the materials was thus determined from the CO_2 adsorption isotherms collected at 273 K and 195 K. The latter, in particular, is considered a reliable method given that the saturation pressure of carbon dioxide at this temperature is 1 atm, which is the same as for N_2 at 77 K.[29] The surface areas calculated using the isotherms at these two temperatures yield congruent results, as shown in Table 1.

At 195 K, the CO_2 uptakes for the POPs synthesized in water, POP-W-Me and POP-W-Et, were found to be 113 $cm^3\ g^{-1}$ and

Table 2 CO_2 uptake at 273 and 298 K (1 bar), and selectivity of CO_2 over N_2 adsorption (IAST at 298 K for a CO_2/N_2 15/85 composition)

POP	CO_2 uptake @273 K $cm^3\ g^{-1}$ (mmol g^{-1})	CO_2 uptake @298 K ($cm^3\ g^{-1}$; mmol g^{-1} STP)	CO_2/N_2 (IAST)
POP-W-Et	38 (1.70)	29 (1.29)	88
POP-W-Me	34 (1.52)	30 (1.34)	69
POP-O-Et	39 (1.74)	33 (1.47)	83
POP-O-Me	30 (1.34)	26 (1.16)	63

145 $cm^3\ g^{-1}$, respectively, accompanied by calculated BET surface areas on the Type-I adsorption curves of 348 $m^2\ g^{-1}$ for POP-W-Me and 389 $m^2\ g^{-1}$ for POP-W-Et (Fig. S26 and 27†). Consistent results were observed for the samples synthesized in organic solvent, POP-O-Me and POP-O-Et, with SA_{BET} values of 302 $m^2\ g^{-1}$ and 440 $m^2\ g^{-1}$, respectively (Fig. S28 and S29†). The CO_2 adsorption at 195 K confirms the porous nature of the materials, albeit the small and less accessible pores pose challenges for N_2 measurements. Additionally, the flexibility of the building units may result in framework swelling, allowing higher and faster adsorption kinetics of CO_2 compared to N_2.[29,30]

Adsorption experiments with CO_2 at 273 K (Fig. S30–S33†) allowed for the assessment of pore size distribution (PSD) using nonlocal density functional theory (NLDFT).[31] The assessment of PSD by CO_2 adsorption at 273 K over N_2 at 77 K is considered more reliable because nitrogen cannot penetrate pores smaller than 5 Å, on the contrary of carbon dioxide that can enter pores in the ultra-microporous region, *i.e.*, ~3.5 Å.[31,32] PSD assessment revealed the coexistence of ultra-micropores of 3.5 Å and micropores of 5.0 Å and 8.0 Å in all the materials (Fig. S38 and S39†), which is typical of microporous polymers.[33]

To evaluate the affinity for CO_2 and the adsorption selectivity over N_2, the uptakes of both gases were measured at 298 K and 1 bar (see *e.g.* Fig. 2 for POP-W-Et) to mimic Vacuum-Swing-Adsorption carbon capture (VSA),[34] which is one of the most common and mildest way to approach CCUS. The CO_2 uptakes at 298 K were lower than that at 195 K but remained consistent for all the investigated materials (30 $cm^3\ g^{-1}$, 26 $cm^3\ g^{-1}$ for POP-W-Me and POP-O-Me; 29 $cm^3\ g^{-1}$, 33 $cm^3\ g^{-1}$ for POP-W-Et and POP-O-Et, see Fig. S38–S41† and Table 2).

The observed difference in adsorption compared to nitrogen suggests the potentially high CO_2 selectivity of these materials over nitrogen. The analysis of CO_2 isotherms at 273 and 298 K allows for the calculations of the isosteric heats of adsorption (Q_{st}). The isotherms were fitted with the Langmuir–Freundlich equation, and the Q_{st} was determined using the Clausius–Clapeyron equation.[35] The Q_{st} for each material were in the 30–35 kJ mol^{-1} range at low coverage, thus following a physisorption-based model (see Fig. S40†). The Q_{st} of CO_2 can be ascribed to the interactions between its quadrupole moment and the POPs, which results in its selective adsorption compared to nitrogen. These values are indicative of a high affinity of the investigated materials for CO_2 but, at the same time, show that the carbon dioxide is not adsorbed too tightly in the pores, making the subsequent desorption less energetically demanding.[36]

Since the amount of CO_2 adsorbed largely exceeds the amount of N_2 adsorbed at the same temperature, we calculated the selectivity of these materials for their potential use in post-combustion separation processes.[37] The fit of the adsorption curves with the IAST method using the IAST++ software[38] allowed us to calculate the ideal selectivity, assuming a 15% CO_2 and 85% N_2 gas mixture, which simulates the typical flue gas composition during post-combustion carbon capture.[39] At pressure equal to 1 bar, POP-W-Et is slightly more selective than POP-W-Me (88 *vs.* 69). It has to be noted that the selectivity of POP-O-Et and POP-O-Me (83 and 63, respectively) are very close to those obtained with the materials synthesized in aqueous media (Fig. 2 and Table 2).

As a summary and analysis of the reported textural properties we can assess that the bulkier ethyl group in POP-Et, compared to the methyl group in POP-Me, likely acts as a more effective spacer between polymer chains, leading to higher BET surface areas (440 and 302 $m^2\ g^{-1}$ for POP-O-Et and POP-O-Me, respectively; Table 1). POP-Et exhibits superior CO_2 uptake than POP-Me (1.74 *vs.* ~1.34 mmol g^{-1} at 273 K, and 1.47 *vs.* ~1.16 mmol g^{-1} at 298 K), and this is combined with a higher CO_2/N_2 selectivity (83 *vs.* 63, as shown in Table 2 and Fig. 2c and d). In terms of solvent effects, no significant differences in textural properties were observed when synthesizing the same polymer in water *versus* an organic solvent. The slight improvement in CO_2 uptake in the organic medium (see 1.47 *vs.* 1.16 mmol g^{-1} for POP-O-Et *vs.* POP-O-Me, Table 2) is expected due to the organic nature of the polymer backbone. However, the water-synthesized polymers display similar textural properties, making the water-based synthesis advantageous due to its greener and more sustainable nature. The pore size distribution, calculated *via* NLDFT from CO_2 adsorption data at 273 K, supports these findings. Fig. S34–S35† demonstrate that both POP-W-Et and POP-O-Et have a higher fraction of ultramicropores centred at 3.5 Å compared to POP-W-Me and POP-O-Me, easily correlating with the higher surface area of the ethyl-substituted polymers. This observation holds for polymers synthesized in both aqueous and organic media and also helps explaining the enhanced CO_2 selectivity of the POP-Et polymers. A detailed analysis of the CO_2 adsorption and desorption isotherms at different temperatures (195–298 K, Fig. S26–S39†) reveals that both POP-Et and POP-Me polymers, regardless of the synthesis medium, exhibit significant hysteresis during CO_2 desorption, particularly evident at 195 K. This consistency across synthesis conditions confirms the reproducibility of both preparation methods. POP-Et displays a more pronounced hysteresis compared to POP-Me, highlighting its enhanced affinity for CO_2. This observation is further supported by the higher isosteric heat of adsorption (Q_{st}) of POP-Et (37 kJ mol^{-1}) compared to POP-Me (31 kJ mol^{-1}), as shown in Fig. S40.† The stronger affinity for CO_2 in POP-Et suggests that the polymer swells more during adsorption, making the desorption in vacuum conditions more difficult. While this hysteresis effect is more prominent at 195 K, it is also observable at higher temperatures (273 and 298 K), albeit to a lesser degree.

Experimental

Details on materials, methods, and characterization techniques are reported in the ESI material.†

Synthesis in water (POP-W-Me/POP-W-Et)

0.4 mmol of the starting tris-amine (*i.e.* 84 mg of $MeNH_2$ and 100 mg of $EtNH_2$ for POP-W-Me and POP-W-Et, respectively) were dissolved in 10 mL of distilled water in a glass scintillation vial (20 mL) provided with screw cap. The mixture was sonicated

for 5 minutes and then 0.4 mmol (84 mg) of TFP were added. The suspension was sonicated for additional 5 minutes to form a homogenous dispersion. The suspension was stirred for 72 h at 70 °C in the closed vial. The formed solid was filtered on a glass fritted funnel, washed with water and ethanol and then dried under vacuum at 80 °C for 24 hours. The yield of polymerization was 93% for POP-W-Me (136 mg), and 90% POP-W-Et (174 mg).

Synthesis in 1,4-dioxane/mesitylene (POP-O-Me/POP-O-Et)

0.4 mmol of the starting tris-amine (*i.e.* 84 mg of $MeNH_2$ and 100 mg of $EtNH_2$ for POP-W-Me and POP-W-Et, respectively) and 0.4 mmol (84 mg) of TFP were suspended in 7.5 mL of a mixture of 1,4-dioxane/mesitylene 4/1 in a glass scintillation vial (20 mL) provided with screw cap. The mixture was sonicated for 5 minutes, and then 2.5 mL of aqueous AcOH 10.5 M were added. The suspension was then sonicated for an additional 5 minutes to form a homogenous dispersion and then stirred for 72 h at 70 °C. The formed solid was filtered on a glass-fitted funnel, washed with water and ethanol and then dried under vacuum at 80 °C for 24 hours. The yield of the polymerization was 92% for POP-O-Me (135 mg) and 85% for POP-O-Et (164 mg).

Conclusions

In this manuscript, we report two new keto-enamine-linked POPs, which differ only in the presence of methyl or ethyl groups in the triamine precursors. The reported method represents an important step forward, as the synthesis of comparable porous organic polymers or covalent organic frameworks requires catalysts such as acetic acid[21,40] or hydrochloric acid in combination with additional reagents such as sodium nitrite.[41] The protocol not only avoids the use of catalyst or additional additives, but also directly produces (without supercritical drying[42]) a material with permanent porosity, representing an easy and green process that allows to produce CO_2-philic POPs. Moreover, the physico-chemical and CO_2 adsorption properties of the obtained materials have proven to be unaffected by the synthesis in water. This was demonstrated by thorough characterization of the POPs synthesised in water (POP-W-Me/POP-W-Et) and from the classical mixture of organic solvents (POP-O-Me/POP-O-Et), combining gas adsorption experiments, SEM, FTIR spectroscopy, PXRD, solid-state magic angle spinning (MAS) NMR spectroscopy, DSC and TGA. Compared to other CO_2-philic POPs synthesized in aqueous media (see Table S3†),[21–26] POP-W-Me and POP-W-Et are highly competitive, being synthesized in pure water at relatively low temperature (70 °C), without addition of catalysts or other additives, in simple glass vials. Most of the CO_2-philic POPs reported in the literature are synthesized in organic solvents or mixtures, while the syntheses in water are performed at high temperatures (>100 °C), in presence of catalysts or other additives, and/or require sophisticate equipment (*e.g.*, for hydrothermal synthesis).

The reported results turn out to be advantageous also compared to the solvent-free mechanochemical synthesis. The porous materials produced through mechanochemical synthesis, in fact, often exhibit a low performance due to the entrapment of oligomeric impurities within the pores during the grinding process.[19]

The slight decrease in surface areas and the quantity of CO_2 adsorbed in the POP-Me family, compared to that of the POP-Et materials, seems to correlate to the presence of a shorter alkyl chain in the amine precursor. Less bulky groups (Me *vs.* Et) in the polymer structure, in fact, can favour the establishment of π–π and H-bonds interactions within the polymer network. This can promote the partial closure of the polymer pores, making them less accessible to gas penetration, as seen in previous works where aliphatic side chains produced the same effect.[43]

The N-/O-rich POP-W-Me and POP-W-Et also show a high adsorption selectivity for CO_2 over N_2 (up to 88) as calculated with the IAST method at 298 K. The obtained results make these novel POPs promising candidates for greener carbon capture technologies based on solid sorbents. However, there are areas that require refinement and will be central to our future studies. Specifically, we aim to develop more sustainable methods for synthesizing building blocks and to optimize the scaling-up of polymer synthesis with a focus on minimizing water consumption.

Data availability

The data supporting the article Novel CO_2-philic porous organic polymers synthesised in water: a leap towards eco-sustainability have been included as part of the ESI.†

Author contributions

RM and SLC: synthesis and characterization, TGA and DSC. YW, MC: gas adsorption studies, data analysis. CXB, SB: CPMAS, PXRD, elemental analyses. VA: supervision, writing.

Conflicts of interest

There are no conflicts to declare.

Acknowledgements

VA, SLC, RM acknowledge the Cariplo Foundation (MOCA project, grant no. 2019-2090) for financial support. VA and SLC also acknowledge the support from the Ministero dell'Università e della Ricerca (MUR) and the University of Pavia through the program "Dipartimenti di Eccellenza 2023–2027". SB acknowledges Lombardy Region for ''Enhancing Photosynthesis'' grant (2021–2024) for the financial support.

Notes and references

1 (*a*) R. L. Siegelman, E. J. Kim and J. R. Long, *Nat. Mater.*, 2021, **20**, 1060; (*b*) H. Chu, Z. Huang, Z. Zhang, X. Yan, B. Qiu and N. Xu, *Sep. Purif. Technol.*, 2024, **343**, 127153; (*c*)

S. Nagireddi, J. R. Agarwal and D. Vedapuri, *ACS Eng. Au*, 2024, **4**, 22–48.

2 (*a*) F. Meng, Y. Meng, T. Ju, S. Han, L. Lin and J. Jiang, *Renew. Sustain. Energy Rev.*, 2022, **168**, 112902; (*b*) P. Wang, Z. Liu, Z. Pan, J. González-Arias, L. Shang, Y. Wang and Z. Zhang, *Sep. Purif. Technol.*, 2024, **346**, 127252.

3 (*a*) E. Khaki, H. Abyar, M. Nowrouzi, H. Younesi, M. Abdollahi and M. G. Enderati, *Environ. Technol. Innovat.*, 2021, **22**, 101507; (*b*) A. Katare, S. Kumar, S. Kundu, S. Sharma, L. Mohan Kundu and B. Mandal, *ACS Omega*, 2023, **8**, 17511–17522; (*c*) S. Kanehashi and C. A. Scholes, *Front. Chem.*, 2020, **14**, 460; (*d*) Z. Dai and L. Deng, *Sep. Purif. Technol.*, 2024, **335**, 126022; (*e*) M. Monteleone, R. Mobili, C. Milanese, E. Esposito, A. Fuoco, S. La Cognata, V. Amendola and J. C. Jansen, *Molecules*, 2021, **26**, 5557; (*f*) R. Mobili, S. La Cognata, M. Monteleone, M. Longo, A. Fuoco, S. A. Serapian, B. Vigani, C. Milanese, D. Armentano, J. C. Jansen and V. Amendola, *Chem.–Eur. J.*, 2023, **29**, e202301437.

4 (*a*) R. Ben-Mansour, M. A. Habib, O. E. Bamidele, M. Basha, N. A. A. Qasem, A. Peedikakkal, T. Laoui and M. Ali, *Appl. Energy*, 2016, **161**, 225; (*b*) L. B. Hamdy, C. Goel, J. A. Rudd, A. R. Barron and E. Andreoli, *Adv. Mater.*, 2021, **2**, 5843–5880; (*c*) B. Gea, M. Zhanga, B. Hua, D. Wua, X. Zhua, U. Eickerb and R. Wang, *Appl. Energy*, 2024, **355**, 122229.

5 R. Gonzalez-Olmos, A. Gutierrez-Ortega, J. Sempere and R. Nomen, *J. CO_2 Util.*, 2022, **55**, 101791.

6 (*a*) K. Sumida, D. L. Rogow, J. A. Mason, T. M. McDonald, E. D. Bloch, Z. R. Herm, T.-H. Bae and J. R. Long, *Chem. Rev.*, 2012, **112**(2), 724; (*b*) Y. Lin, C. Kong, Q. Zhang and L. Chen, *Adv. Energy Mater.*, 2017, **7**, 1601296; (*c*) H. Demir, G. Onder Aksu, H. Can Gulbalkan and S. Keskin, *Carbon Capture Sci. Technol.*, 2022, **2**, 100026.

7 (*a*) K. Krishnan, J. M. Crawford, P. K. Thallapally and M. A. Carreon, *Ind. Eng. Chem. Res.*, 2022, **61**, 10547–10553; (*b*) W. Wang, K. Su and D. Yuan, *Mater. Chem. Front.*, 2023, **7**, 5247; (*c*) S. La Cognata, R. Mobili, C. Milanese, M. Boiocchi, M. Gaboardi, D. Armentano, J. C. Jansen, M. Monteleone, A. R. Antonangelo, M. Carta and V. Amendola, *Chem.–Eur. J.*, 2022, **28**, e202201631; (*d*) V. Amendola, M. Boiocchi, L. Fabbrizzi and N. Fusco, *Eur. J. Org Chem.*, 2011, **32**, 6434–6444; (*e*) S. La Cognata and V. Amendola, *Chem. Commun.*, 2023, **59**, 13668–13678.

8 (*a*) J. Baltrusaitis, J. Schuttlefield, E. Zeitler and V. H. Grassian, *Chem. Eng. J.*, 2011, **170**(2–3), 471; (*b*) G. Landeta Avellaneda, R. Denoyel and I. Beurroies, *Microporous Mesoporous Mater.*, 2024, **363**, 112801; (*c*) Y. Abdullatif, A. Sodiq, N. Mir, Y. Bicer, T. Al-Ansari, M. H. El-Naasc and A. I. Amhamed, *RSC Adv.*, 2023, **13**, 5687–5722.

9 (*a*) K. S. Song, P. W. Fritz and A. Coskun, *Chem. Soc. Rev.*, 2022, **51**, 9831; (*b*) W. Wang, M. Zhouab and D. Yuan, *J. Mater. Chem. A*, 2017, **5**, 1334; (*c*) S. Fajal, S. Dutta and S. K. Ghosh, *Mater. Horiz.*, 2023, **10**, 4083; (*d*) S. Bracco, D. Piga, I. Bassanetti, J. Perego, A. Comotti and P. Sozzani, *J. Mater. Chem. A*, 2017, **5**, 10328–10337; (*e*) A. Comotti, F. Castiglioni, S. Bracco, J. Perego, A. Pedrini, M. Negroni and P. Sozzani, *Chem. Commun.*, 2019, **5**, 8999–9002; (*f*) W. Song, Y. Tang, B. Y. Moon, Q. Liao, H. Xu, Q. Hou, H. Zhang, D.-G. Yu, Y. Liao and I. Kim, *Green Chem.*, 2024, **26**, 2476–2504.

10 (*a*) H. Li, A. Dilipkumar, S. Abubakar and D. Zhao, *Chem. Soc. Rev.*, 2023, **52**, 6294; (*b*) H. Mabuchi, T. Irie, J. Sakai, S. Das and Y. Negishi, *Chem.–Eur. J.*, 2024, **30**, e202303474; (*c*) H. Lyu, H. Li, N. Hanikel, K. Wang and O. M. Yaghi, *J. Am. Chem. Soc.*, 2022, **144**(28), 12989.

11 (*a*) Z. Hu, Y. Wang, X. Wang, L. Zhai and D. Zhao, *AIChE J.*, 2018, **64**, 3376; (*b*) S. H. Pang, M. L. Jue, J. Leisen, C. W. Jones and R. P. Lively, *ACS Macro Lett.*, 2015, **4**(12), 1415.

12 (*a*) Y. Xie, T.-T. Wang, X.-H. Liu, K. Zou and W.-Q. Deng, *Nat. Commun.*, 2013, **4**, 1960; (*b*) D. Dai, J. Yang, Y.-C. Zou, J.-R. Wu, L.-L. Tan, Y. Wang, B. Li, T. Lu, B. Wang and Y.-W. Yang, *Angew. Chem., Int. Ed.*, 2021, **60**, 8967.

13 (*a*) W. Chen, P. Chen, G. Zhang, G. Xing, Y. Feng, Y.-W. Yang and L. Chen, *Chem. Soc. Rev.*, 2021, **50**, 11684; (*b*) Z. L and Y.-W. Yang, *Adv. Mater.*, 2022, **34**, 2107401.

14 (*a*) J. L. Wu, F. Xu, S. M. Li, P. W. Ma, X. C. Zhang, Q. H. Liu, R. W. Fu and D. C. Wu, *Adv. Mater.*, 2019, **31**, 1802922; (*b*) A. R. Antonangelo, N. Hawkins, E. Tocci, C. Muzzi, A. Fuoco and M. Carta, *J. Am. Chem. Soc.*, 2022, **144**(34), 15581.

15 (*a*) D.-H. Yang, Y. Tao, X. Ding and B.-H. Han, *Chem. Soc. Rev.*, 2022, **51**, 761; (*b*) G. Ji, Y. Zhao and Z. Liu, *Green Chem.*, 2022, **3**(2), 96; (*c*) T. Zhang, G. Xing, W. Chen and L. Chen, *Mater. Chem. Front.*, 2020, **4**, 332.

16 (*a*) Z. Li and Y.-W. Yang, *Adv. Mater.*, 2022, **34**, 2107401; (*b*) S. Wang, H. Li, H. Huang, X. Cao, X. Chen and D. Cao, *Chem. Soc. Rev.*, 2022, **51**, 2031.

17 (*a*) X. Liu, C.-F. Liu, W.-Y. Lai and W. Huang, *Adv. Mater. Technol.*, 2020, **5**, 2000154; (*b*) H. Liao, G. Liao, Q. Yang, Y. Xiao, B. Cheng and S. Lei, *J. Energy Storage*, 2024, **82**, 110520.

18 (*a*) P. Bhanja, A. Modak and A. Bhaumik, *ChemCatChem*, 2019, **11**, 244; (*b*) J. Deng, Z. Dai and L. Deng, *J. Membr.*, 2020, **610**, 118262.

19 (*a*) S. Kandambeth, A. Mallick, B. Lukose, M. V. Mane, T. Heine and R. Banerjee, *J. Am. Chem. Soc.*, 2012, **134**, 19524–19527; (*b*) S. Kandambeth, K. Dey and R. Banerjee, *J. Am. Chem. Soc.*, 2019, **141**(5), 1807–1822; (*c*) B. P. Biswal, S. Chandra, S. Kandambeth, B. Lukose, T. Heine and R. Banerjee, *J. Am. Chem. Soc.*, 2013, **135**, 5328–5331; (*d*) J. Perego, D. Piga, S. Bracco, P. Sozzani and A. Comotti, *Chem. Commun.*, 2018, **54**, 9321–9324.

20 (*a*) D. Kaleeswaran, P. Vishnoi and R. Murugavel, *J. Mater. Chem. C*, 2015, **3**, 7159–7171; (*b*) R. Gomes and A. Bhaumi, *RSC Adv.*, 2016, **6**, 28047–28054.

21 D. Luo, T. Shi, Q.-H. Li, Q. Xu, M. Strømme, Q.-F. Zhang and C. Xu, *Angew. Chem., Int. Ed.*, 2023, **62**, e202305225.

22 J. Thote, H. B. Aiyappa, R. R. Kumar, S. Kandambeth, B. P. Biswal, D. B. Shinde, N. C. Royd and R. Biswaee, *IUCrJ*, 2016, **3**, 402.

23 J. A. Martìn-Illàn, D. Rodrìguez-San-Miguel, C. Franco, I. Imaz, D. Maspoch, J. Puigmartì-Luis and F. Zamora, *Chem. Commun.*, 2020, **56**, 6704.
24 L. Guo, Q. Y. Zhang, Z. Yu, R. Krishna and F. Luo, *Chem. Mater.*, 2023, **35**(14), 5648.
25 (*a*) M. Lahnsteiner, M. Caldera, H. M. Moura, D. A. Cerron-Infantes, J. Roeser, T. Konegger, A. Thomas, J. Menche and M. M. Unterlass, *J. Mater. Chem. A*, 2021, **9**, 19754–19769; (*b*) B. Baumgartner, M. Puchberger and M. M. Unterlass, *Polym. Chem.*, 2015, **6**, 5773–5781.
26 G. Ji, Z. Yang, H. Zhang, Y. Zhao, B. Yu, Z. Ma and Z. Liu, *Angew. Chem., Int. Ed.*, 2016, **55**, 9685–9689.
27 J. Lu, F. Lin, Q. Wen, Q.-Y. Qi, J.-Q. Xu and X. Zhao, *New J. Chem.*, 2019, **43**, 6116.
28 S. Chandra, S. Kandambeth, B. P. Biswal, B. Lukose, S. M. Kunjir, M. Chaudhary, R. Babarao, T. Heine and R. Banerjee, *J. Am. Chem. Soc.*, 2013, **135**, 17853–17861.
29 K. C. Kim, T. U. Yoon and Y. S. Bae, *Microporous Mesoporous Mater.*, 2016, **224**, 294.
30 M. Chen, B. Coasne, R. Guyer, D. Derome and J. Carmeliet, *Nat. Commun.*, 2018, **9**, 3507.
31 (*a*) M. Thommes, K. Kaneko, A. V. Neimark, J. P. Olivier, F. Rodriguez-Reinoso, J. Rouquerol and K. S. W. Sing, *Pure Appl. Chem.*, 2015, **87**, 1051; (*b*) M. Thommes and K. A. Cychosz, *Adsorption*, 2014, **20**, 233.
32 (*a*) D. Lozano-Castelló, D. Cazorla-Amorós and A. Linares-Solano, *Carbon*, 2004, **42**, 1233; (*b*) K. A. Cychosz and M. Thommes, *Engineering*, 2018, **4**, 559.
33 (*a*) R. Tan, A. Wang, R. Malpass-Evans, R. Williams, E. W. Zhao, T. Liu, C. Ye, X. Zhou, B. P. Darwich, Z. Fan, L. Turcani, E. Jackson, L. Chen, S. Y. Chong, T. Li, K. E. Jelfs, A. I. Cooper, N. P. Brandon, C. P. Grey, N. B. McKeown and Q. Song, *Nat. Mater.*, 2020, **19**, 195; (*b*) C. Soto, N. Cicuttin, F. J. Carmona, M. de la Viuda, A. Tena, Á. E. Lozano, A. Hernández, L. Palacio and P. Prádanos, *J. Membr.*, 2023, **683**, 121841.
34 (*a*) H. Zhang, Z. Zhou, Y. Yin, *et al.*, *EcoEnergy*, 2023, **1**(2), 217; (*b*) M. Chawla, H. Saulat, M. Masood Khan, M. Mahmood Khan, S. Rafiq, L. Cheng, T. Iqbal, M. I. Rasheed, M. Z. Farooq, M. Saeed, N. M. Ahmad, M. B. Khan Niazi, S. Saqib, F. Jamil, A. Mukhtar and N. Muhammad, *Chem. Eng. Technol.*, 2020, **43**, 184; (*c*) K. A. Fayemiwo, G. T. Vladisavljević, S. A. Nabavi, B. Benyahia, D. P. Hanak, K. N. Loponov and V. Manović, *Chem. Eng. J.*, 2018, **334**, 2004.
35 K. Wang, S. Qiao and X. Hu, *Sep. Purif. Technol.*, 2004, **34**, 165–176.
36 L. W. Bruch, *Surf. Sci.*, 1983, **125**(1), 194.
37 H. Zhou, C. Rayer, A. R. Antonangelo, N. Hawkins and M. Carta, *ACS Appl. Mater. Interfaces*, 2022, **14**, 20997–21006.
38 S. Lee, J. H. Lee and J. Kim, *Korean J. Chem. Eng.*, 2018, **35**, 214–221.
39 K. T. Leperi, R. Q. Snurr and F. You, *Ind. Eng. Chem. Res.*, 2016, **55**, 3338–3350.
40 I. Martínez-Visus, M. Ulcuango, B. Zornoza, J. Coronas and C. Téllez, *Chem.–Eur. J.*, 2023, **29**, e202203907.
41 (*a*) L. Huang, M. He, B. Chen, Q. Cheng and B. Hu, *ACS Sustainable Chem. Eng.*, 2017, **5**, 4050–4055; (*b*) Y. Shen, W.-X. Ni and B. Li, *ACS Omega*, 2021, **6**, 3202–3208.
42 M. Avais and S. Chattopadhyay, *ACS Appl. Polym. Mater.*, 2021, **3**, 789–800.
43 (*a*) B. S. Ghanem, M. Hashem, K. D. M. Harris, K. J. Msayib, M. Xu, P. M. Budd, N. Chaukura, D. Book, S. Tedds, A. Walton and N. B. McKeown, *Macromolecules*, 2010, **43**(12), 5287; (*b*) R. Swaidan, M. Al-Saeedi, B. Ghanem, E. Litwiller and I. Pinnau, *Macromolecules*, 2014, **47**(15), 5104.